UC Davis

Title

NLRs derepress MED10b- and MED7-mediated repression of jasmonate-dependent transcription to activate immunity.

Permalink

https://escholarship.org/uc/item/4jx2m51p

Journal

Proceedings of the National Academy of Sciences of USA, 120(28)

Authors

Wu, Qian
Tong, Cong
Chen, Zhengqiang
et al.

Publication Date

2023-07-11

DOI

10.1073/pnas.2302226120

Peer reviewed

NLRs derepress MED10b- and MED7-mediated repression of jasmonate-dependent transcription to activate immunity

Qian Wu[a], Cong Tong[a], Zhengqiang Chen[a], Shen Huang[a], Xiaohui Zhao[b], Hao Hong[a], Jia Li[a] [ID], Mingfeng Feng[a] [ID], Huiyuan Wang[a,c], Min Xu[a], Yuling Yan[a] [ID], Hongmin Cui[a], Danyu Shen[a], Gan Ai[a], Yi Xu[a] [ID], Junming Li[d], Hui Zhang[e], Changjun Huang[f], Zhongkai Zhang[g], Suomeng Dong[a] [ID], Xuan Wang[a] [ID], Min Zhu[a], Savithramma P. Dinesh-Kumar[h] [ID], and Xiaorong Tao[a,1] [ID]

Plant intracellular nucleotide-binding domain, leucine-rich repeat-containing receptors (NLRs) activate a robust immune response upon detection of pathogen effectors. How NLRs induce downstream immune defense genes remains poorly understood. The Mediator complex plays a central role in transducing signals from gene-specific transcription factors to the transcription machinery for gene transcription/activation. In this study, we demonstrate that MED10b and MED7 of the Mediator complex mediate jasmonate-dependent transcription repression, and coiled-coil NLRs (CNLs) in *Solanaceae* modulate MED10b/MED7 to activate immunity. Using the tomato CNL *Sw-5b*, which confers resistance to *tospovirus*, as a model, we found that the CC domain of Sw-5b directly interacts with MED10b. Knockout/down of *MED10b* and other subunits including *MED7* of the middle module of Mediator activates plant defense against *tospovirus*. MED10b was found to directly interact with MED7, and MED7 directly interacts with JAZ proteins, which function as transcriptional repressors of jasmonic acid (JA) signaling. MED10b–MED7–JAZ together can strongly repress the expression of JA-responsive genes. The activated Sw-5b CC interferes with the interaction between MED10b and MED7, leading to the activation of JA-dependent defense signaling against *tospovirus*. Furthermore, we found that CC domains of various other CNLs including helper NLR NRCs from *Solanaceae* modulate MED10b/MED7 to activate defense against different pathogens. Together, our findings reveal that MED10b/MED7 serve as a previously unknown repressor of jasmonate-dependent transcription repression and are modulated by diverse CNLs in *Solanaceae* to activate the JA-specific defense pathways.

Mediator complex | NLRs | Sw-5b | effector-triggered immunity

Plants use two tiers of innate immune system known as the pattern-triggered immunity (PTI) and the effector-triggered immunity (ETI) to defend against microbial pathogens (1, 2). The PTI is initiated by cell-surface pattern recognition receptors upon recognition of microbe-associated molecular patterns (3–5), whereas the ETI is initiated by intracellular nucleotide-binding leucine-rich repeat-containing receptors (NLRs) upon recognition of pathogen effectors (1, 2, 6, 7). The PTI-induced plant defense is often mild and transient, whereas the defense by ETI is robust and persistent (6). The downstream defense outputs of PTI and ETI largely overlap (8, 9), and the PTI can boost the ETI defense signaling (10, 11).

NLRs contain an N-terminal coiled-coil (CC) or a Toll/interleukin-1 receptor (TIR) homology domain, a nucleotide-binding adaptor shared by Apaf-1, certain resistance proteins, CED-4 domain (NB-ARC), and a leucine-rich repeat domain (2, 12). Upon recognition of the pathogen effectors directly or indirectly, the NLRs switch from the ADP-bound (inactive) state to the ATP-bound (active) state (13, 14). The activated NLRs then induce robust downstream defense response, which is typically associated with ROS production, influx of calcium, and other responses that culminate into hypersensitive response (HR) cell death (6). Recently, it was shown that activated Arabidopsis CC–type NLR (CNL) ZAR1 assembles into a pentamer structure called resistosome and associate with the plasma membrane to function as a calcium-permeable cation channel to trigger cell death and immunity (15, 16). It was also reported recently that the TIR-containing NLR (TNL) proteins can catalyze NAD^+ and produce two types of signaling molecules that selectively activate EDS1–SAG101 and EDS1–PAD4 modules. The two EDS1 signaling modules then activate the helper NLRs AtADR1 and AtNRG1, respectively (17, 18). Recently, the AtADR1 and AtNRG1 were also found to function as calcium-permeable cation channels in triggering cell death (19). Despite this, cell death is not sufficient to restrict the spread of pathogen (20, 21). Even when the plant induced cell death, the plant still get

Significance

Jasmonic acid (JA) plays an important role in plant defense against insects, pathogenic fungi and viruses mediated by cell-surface pattern recognition receptors, and intracellular nucleotide-binding leucine-rich repeat (NLR) class immune receptors. In this study, we uncovered a previously unknown role for MED10b and MED7 of the Mediator complex in the jasmonate-dependent transcription response, and coiled-coil NLRs (CNLs) in *Solanaceae* modulate MED10b/MED7 to activate immunity. MED10b, MED7, and transcription repressor JAZs interact with each other to repress the expression of jasmonate-dependent defense genes. Whereas, CC domains of Sw-5b and various other CNLs from *Solanaceae* interfere with the interaction between MED10b and MED7 thereby derepressing the repressor activity of MED10b–MED7–JAZ to activate immunity.

infected by pathogen. In addition to HR cell death, NLRs can also induce major transcriptome reprogramming of nuclear genes that play a role in defense (6). However, how NLRs upon pathogen recognition induce the expression of defense-related genes remains largely unknown.

Mediator is a multiprotein complex that plays a central role in gene transcription/activation in eukaryotes. The Mediator serves as a molecular bridge to link transcription factors to RNA polymerase II (Pol II) (22, 23). The Mediator complex transduces signals from gene-specific transcription factors to the transcription machinery to activate target gene expression (22, 23). During transcription initiation, transcription factors bind to the promoters of specific genes and recruit the Mediator complex. The Mediator complex then recruits Pol II to the promoters to form the transcriptional preinitiation complexes (24, 25). Yeast and animal Mediator complexes are known to contain about 25 and 31 subunits, respectively. Plant Mediator complex includes approximately 34 subunits (26). The core Mediator complex and the head, middle, and tail modules are well conserved in yeast, animals, and plants. As the master coordinators of gene transcription, the Mediator complex participates in many signaling pathways, including those involved in cell division, cell fate, organogenesis, hormone-associated responses, and plant immunity (27, 28).

Jasmonic acid (JA) plays a crucial role in regulating various plant stress responses including insect defense and pathogen resistance (29, 30). MYELOCYTOMATOSIS 2/3/4 (MYC2/3/4) transcription factors, which belong to bHLH transcription factor family, are the core transcription activators of JA response genes. The transcriptional repressor JASMONATE ZIM DOMAIN (JAZ) proteins physically associate with MYC2/3/4 and inhibit the activation of these transcription factors. At the same time, JAZ proteins recruit the transcriptional corepressor TOPLESS (TPL) directly or through interacting with EAR motif–containing adapter protein NINJA, another corepressor, to further inhibit the activation of MYC2/3/4 (31, 32). It remains unknown yet whether any other transcriptional corepressor works together with JAZ proteins to repress the transcription of JA-dependent defense genes.

Not only does JA play an important role in regulating plant defense responses against necrotrophic, biotrophic, and hemibiotrophic pathogens (33–35), several recent studies also showed that JA signaling plays an important role in plant defense against viruses. Silencing the JA biosynthesis gene allene oxide cyclase (*AOC*) increases plant susceptibility to *Turnip mosaic virus* (TuMV) in *Nicotiana benthamiana* (36). Application of methyl jasmonate (MeJA) significantly reduces the infection of *Rice black–streaked dwarf virus* (RBSDV) in rice, while a Rice *OsCOI1* RNAi line (*coi1-13*) is more susceptible to RBSDV (37). Overexpression of OsMYC2 or OsMYC3 increases plant resistance to *Rice stripe virus* (RSV) or *Southern rice black–streaked dwarf virus* (SRBSDV), whereas *osmyc2* or *osmyc3* mutant shows increased plant susceptibility to RSV or SRBSDV (38, 39).

Tomato spotted wilt orthotospovirus (TSWV) is among the most destructive plant viruses (40) and causes significant economic losses annually, posing serious threats to global food security (41, 42). Tomato resistance gene *Sw-5b* is the most effective resistance gene to control TSWV infection (43, 44) and has been widely used in tomato-breeding projects (45, 46). The *Sw-5b* belongs to CNL, and many CNLs including *R8*, *Mi-1.2*, *Rpi-blb2*, and *Rx* have been characterized in solanaceous plants. However, little is known about how these *solanaceae* NLRs induce downstream immunity. *N. benthamiana* is an ideal model plant for plant–microbe interaction studies (47). Many NLRs, including *Sw-5b*

in the family of *Solanaceae,* can provide strong immunity to their cognate pathogens when those NLRs were expressed in *N. benthamiana* (48). This indicates that the downstream immune signaling controlled by those NLRs is conserved in *N. benthamiana* and other solanaceous plants.

In this study, we used tomato *Sw-5b* and various solanaceous CNLs and *N. benthamiana* as our assay model. We demonstrated that the CC domains of Sw-5b and other CNLs can interact directly with the Mediator 10b (MED10b), a subunit in the middle module of the Mediator complex. We found that MED10b–MED7–JAZ proteins interact with each other and corepress jasmonate-specific defense gene expressions. The CC domains of Sw-5b and other CNLs including NRC helper NLRs can interfere with the interaction between MED10b and MED7, therefore derepressing the repressor activity of MED10b–MED7–JAZ proteins on JA-dependent defense gene expressions. Our findings uncovered a previously unknown role for MED10b/MED7 in jasmonate-dependent transcription response, and CNLs in *Solanaceae* modulate MED10b/MED7 to activate immunity.

Results

Sw-5b CC Domain Directly Interacts with MED10b. The CC domain of several CNLs has been shown to play critical role in the activation of downstream immune signaling (49–53). To test whether the CC domain of Sw-5b NLR can activate immune defense against *tospovirus*, we coexpressed the Sw-5b CC domain with the previously reported TSWV infectious replicons ($L_{(+)opt}$+$M_{(-)opt}$+$SR_{(+)eGFP}$) (54) in *N. benthamiana* leaves through agro-infiltration. The expression of Sw-5b CC domain alone in *N. benthamiana* leaves did not cause cell death (*SI Appendix,* Fig. S1*A*). However, coexpression of FLAG-Sw-5b-CC significantly inhibited eGFP expression from $L_{(+)opt}$+$M_{(-)opt}$+$SR_{(+)eGFP}$ viral replicon compared to the leaves coexpressing $L_{(+)opt}$+$M_{(-)opt}$+$SR_{(+)eGFP}$ and the empty vector (EV) (*SI Appendix,* Fig. S1 *B* and *C*). These results indicate that CC domain can induce a defense response against TSWV.

To elucidate the downstream components involved in the Sw-5b CC domain–induced immune signaling, we used the CC domain as a bait to screen its interacting proteins through a yeast two-hybrid (Y2H) screening using cDNA library from *N. benthamiana*. The Mediator 10b (*Nb*MED10b), a subunit in the middle module of Mediator complex (55), was identified as the CC-interacting protein (Fig. 1*A* and *SI Appendix,* Fig. S2*A*). The GST pull-down, coimmunoprecipitation (Co-IP), and bimolecular fluorescence complementation (BiFC) assay results confirmed that CC domain interacts with *Nb*MED10b in vitro and in planta (Fig. 1 *B* and *C* and *SI Appendix,* Fig. S2*B*). The Y2H result also showed that the autoactive mutant of full-length Sw-5b^{D857V} (21) interacted strongly with *Nb*MED10b (Fig. 1*D*). In contrast, the Sw-5b^{K568R}, a P-loop defective mutant that does not induce HR in plants (21), failed to interact with *Nb*MED10b (Fig. 1*D*). These interactions were confirmed by the result from BiFC assays (Fig. 1*E*).

MED10b Negatively Regulates Sw-5b-Mediated Defense. To elucidate the function of *NbMED10b* in *Sw-5b*-mediated resistance, we silenced *NbMED10b* expression in the *Sw-5b* transgenic *N. benthamiana* plants (56) through virus-induced gene silencing (VIGS) using a *Tobacco rattle virus* (TRV) (*SI Appendix,* Figs. S3 and S4). Three weeks post-TRV treatment, the TRV-*NbMED10b*-treated (referred to as *NbMED10b*-silenced) plants or the TRV-*GUS* (nonsilenced) control plants were inoculated with the TSWV $L_{(+)opt}$+$M_{(-)opt}$+$SR_{(+)eGFP}$ clones via agro-infiltration. The
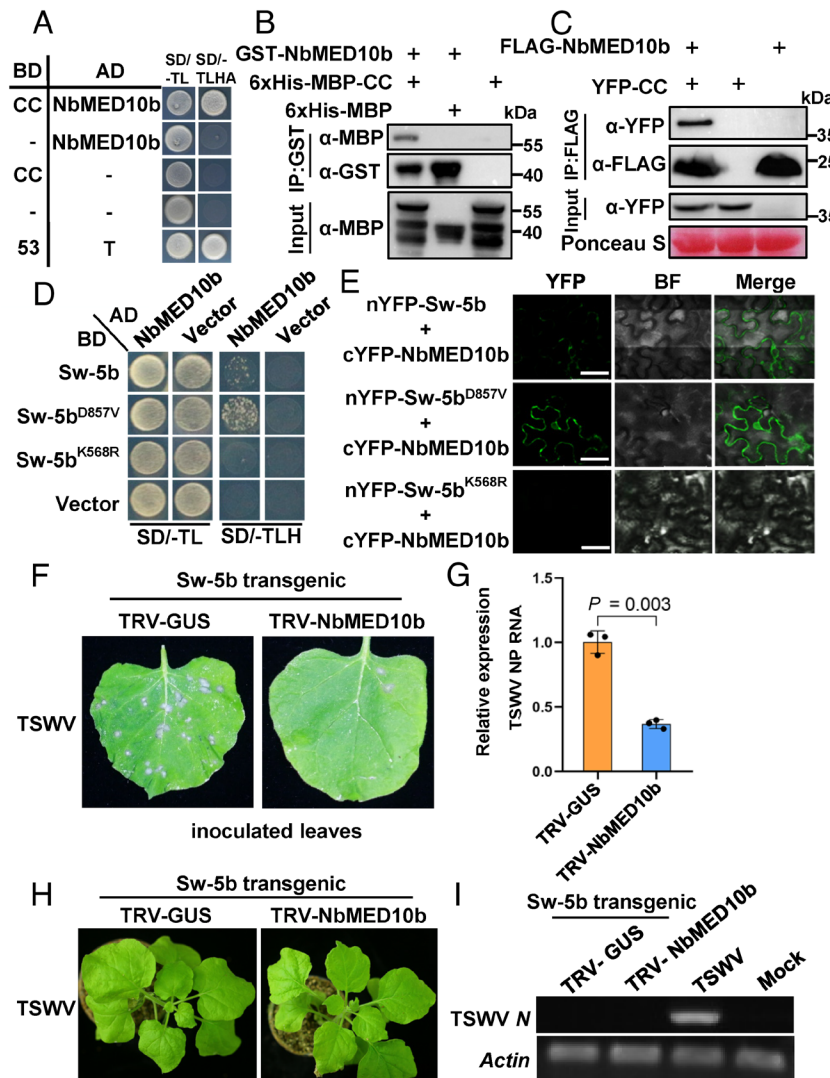
Fig. 1. Sw-5b CC domain interacts with *Nb*MED10b, a negative regulator of the Sw-5b-mediated defense against TSWV infection. (*A*) A yeast two-hybrid (Y2H) assay result showing an interaction between *Nb*MED10b and Sw-5b CC domain. The transformed yeast cultures were grown on the solid SD dropout medium lacking Trp and Leu (SD/-TL) and the dropout medium lacking Trp, Leu, His, and Ade (SD/-TLHA), respectively. (*B*) A GST pull-down assay result showing the interaction between the GST-*Nb*MED10b and 6×His-MBP–Sw-5b-CC. 6×His-MBP–Sw-5b-CC, 6×His-MBP, and GST-*Nb*MED10b were expressed individually in *Escherichia coli* and then purified. The purified 6×His-MBP–Sw-5b-CC or 6×His-MBP was incubated with GST-*Nb*MED10b followed by the pull-down assay using glutathione-sepharose beads. The blots were probed with an anti-GST- or anti-MBP-specific antibody. (*C*) A coimmunoprecipitation (Co-IP) assay for the interaction between *Nb*MED10b and the Sw-5b CC domain. FLAG-*Nb*MED10b was coimmunoprecipitated with YFP-CC from *N. benthamiana* leaf extracts. The blots were then probed using an anti-FLAG or an anti-YFP antibody. (*D*) A Y2H assay result showing the interaction between *Nb*MED10b and Sw-5b, Sw-5b^D857V, or Sw-5b^K568R mutant. The transformed yeast cultures were grown on the SD/-TL and the SD/-TLH dropout plates, respectively. (*E*) Bimolecular fluorescence complementation (BiFC) assay results showing the interaction between *Nb*MED10b and Sw-5b, Sw-5b^D857V, or Sw-5b^K568R mutant. The nYFP- or cYFP-tagged proteins were transiently coexpressed in *N. benthamiana* leaf cells and then imaged under confocal microscopy. The YFP signal is shown in green (Scale bars, 20 μm.). (*F*) The *NbMED10b*-silenced or nonsilenced *Sw-5b* transgenic *N. benthamiana* plant leaves were inoculated with TSWV-infected crude leaf extracts. The TSWV-inoculated leaves were photographed at 3 d post TSWV inoculation (dpi) to show the number of HR loci. (*G*) The accumulation level of TSWV RNA in the inoculated leaves shown in (*F*) was determined through qRT-PCR using TSWV *N* gene–specific primers. All the inoculated leaves were harvested at 3 dpi. The expression levels of *NbActin* in these assayed leaf samples were used as the internal control. Data are presented as the means ± SE (three biological samples per treatment). (*H*) Phenotype of systemic leaves of the *NbMED10b*-silenced and nonsilenced *Sw-5b* transgenic *N. benthamiana* plants inoculated with TSWV. The plants were photographed at 14 dpi. (*I*) RT-PCR detection of TSWV RNA in the systemic leaves of the plants shown in the panel (*H*) at 14 dpi using TSWV *N* gene–specific primers. The crude extract from a TSWV-infected *N. benthamiana* leaf sample was used as the positive control. The leaf sample from a mock-inoculated *Sw-5b* transgenic *N. benthamiana* plant was used as the negative control. The expression levels of *NbActin* in the assayed samples were used as the internal controls.

results showed that, compared to the nonsilenced control plants, the *NbMED10b*-silenced *Sw-5b* transgenic *N. benthamiana* plants accumulated much less eGFP expressed from TSWV (*SI Appendix,* Fig. S4 *A* and *B*). When the *NbMED10b*-silenced or nonsilenced plants were rub-inoculated with TSWV-infected leaf extracts, it induced numerous HR loci in the nonsilenced *Sw-5b* transgenic plant leaves (Fig. 1*F*). In contrast, TSWV inoculation caused very few HR loci in the *NbMED10b*-silenced *Sw-5b* transgenic plant leaves (Fig. 1*F*). Generally, even with HR, certain level of viral accumulation including replication and intercellular movement

of the virus occurs. Complete absence of HR cell death in *NbMED10b*-silenced *Sw-5b* transgenic plant leaves resembles the phenotype of extreme resistance observed in the case of some *R* genes which no longer allow viral accumulation during defense response (57, 58). Analysis of TSWV-inoculated leaves through qRT-PCR showed that the accumulation level of viral RNA in the TSWV-inoculated *NbMED10b*-silenced leaves was significantly reduced compared to that in the TSWV-inoculated nonsilenced leaves (Fig. 1*G*). In addition, we also examined whether silencing *NbMED10b* has any effect on TSWV systemic infection in *Sw-5b*

transgenic plant. No TSWV was detected in the newly emerged systemic leaves of the *NbMED10b*-silenced plants (Fig. 1 *H* and *I*).

We then examined the interaction between Sw-5b CC and *Sl*MED10b from tomato. The results of Y2H and Co-IP assays showed that the Sw-5b CC domain interacted with *Sl*MED10b in vitro and in planta (*SI Appendix,* Fig. S5 *A* and *B*). We silenced *SlMED10b* expression in tomato cv. IVF3545 plants (with *Sw-5b* gene) followed by inoculation with TSWV (*SI Appendix,* Fig. S5 *C* and *D*). Similar to transgenic *N. benthamiana* with *Sw-5b*, the numbers of HR loci and the accumulation level of TSWV RNA in the TSWV-inoculated leaves of the *SlMED10b*-silenced tomato plants were significantly reduced compared to the control plants (*SI Appendix,* Fig. S5 *E* and *F*). In addition, no systemic TSWV infection was detected in the newly emerged systemic leaves of the TSWV-inoculated *SlMED10b*-silenced tomato plants (*SI Appendix,* Fig. S5 *G* and *H*). These results indicate that MED10b functions as a negative regulator of Sw-5b-mediated immune response to TSWV.

Knockout/down of *NbMED10b* and Other Subunits in the Middle Module of Mediator Complex Activate Defense against TSWV Infection. To further investigate how *MED10b* negatively regulates resistance, we generated *med10b* knockout mutant lines in wild-type *N. benthamiana* using CRISPR/Cas9-based technology (*SI Appendix,* Fig. S6 *A–C*). Compared to the wild-type plants, the *Nbmed10b* knockout mutant plants showed a strong dwarfing phenotype (Fig. 2*A* and *SI Appendix,* Fig. S6*D*). The *Nbmed10b* knockout plants were rub-inoculated with TSWV-infected leaf extracts. The accumulation level of TSWV RNA in the leaves of the *Nbmed10b* knockout plants was significantly reduced (Fig. 2*B*), suggesting that knockout of *NbMED10b* activated plant defense against TSWV infection. As *Nbmed10b* knockout caused strong dwarfing phenotype, we also silenced *NbMED10b* expression in wild-type *N. benthamiana* plants through TRV-mediated gene silencing followed by inoculation of TSWV L$_{(+)opt}$+M$_{(-)opt}$+SR$_{(+)}$ $_{eGFP}$ infectious clone or TSWV-containing sap. Similar to the above results, the accumulation of TSWV was significantly lower in the leaves of the *NbMED10b*-silenced plants compared to the control plants (Fig. 2 *C* and *D* and *SI Appendix,* Fig. S7). Next, we silenced *SlMED10b* expression in tomato cv. Moneymaker (without *Sw-5b*) through VIGS followed by TSWV inoculation (*SI Appendix,* Fig. S8 *A* and *B*). The results showed that the accumulation level of TSWV RNA was also significantly reduced in leaves of the *SlMED10b*-silenced tomato plants (*SI Appendix,* Fig. S8 *C* and *D*).

As knockout/down *MED10b* lead to immune activation, we then analyzed the role of other subunits in the middle module of the Mediator complex, i.e., *NbMED1, NbMED4, NbMED7, NbMED9, NbMED21, NbMED26,* and *NbMED31* through VIGS (Fig. 2*E*). The expressions of *NbMED1, NbMED4, NbMED7, NbMED9, NbMED21, NbMED26,* and *NbMED31* in *N. benthamiana* plants were silenced individually using the TRV-based VIGS vectors (*SI Appendix,* Fig. S9 *A* and *B*) followed by inoculation of TSWV replicon via agro-infiltration. Strikingly, silencing the expressions of *NbMED1, NbMED4, NbMED7, NbMED9, NbMED21,* and *NbMED26* also suppressed the accumulation of TSWV replicon (Fig. 2 *F* and *G*), indicating that knockdown of expression of these subunits in the middle module of Mediator complex can also activate plant defense against TSWV infection.

We also analyzed whether subunits in the head and the tail module of Mediator complex have any effect against TSWV. The expressions of *NbMED11* and *NbMED18* in the head module and those of *NbMED15* and *NbMED23* in the tail module were silenced through VIGS (*SI Appendix,* Fig. S9 *A* and *B*). The results showed that, unlike *NbMED10b* or other subunits in the middle module,

silencing of *NbMED11, NbMED18, NbMED15,* or *NbMED23* had no effect on TSWV accumulation (Fig. 2 *F* and *G*).

MED10b Directly Interacts with MED7, Which Also Negatively Regulates Sw-5b-Mediated Defense. Based on the above results, we hypothesized that MED10b may interact with other subunit(s) of the middle module of Mediator complex to function as repressors of plant defense against TSWV. Whereas, binding of Sw-5b CC domain to MED10b might disrupt the interaction between MED10b with its adjacent subunit(s) in the middle module of Mediator complex and consequently derepresses the repressor activity of those subunits, leading to an activation of host defense against TSWV infection. To test this hypothesis, we examined the interactions between *Nb*MED10b and other three subunits, *Nb*MED7, *Nb*MED26, and *Nb*MED31, that were predicted to be in close proximity to *Nb*MED10b in the middle module (59) (Fig. 2*E*). The results of BiFC assay showed that *Nb*MED10b could interact with *Nb*MED7, *Nb*MED26, or *Nb*MED31 (*SI Appendix,* Fig. S10*A*). However, the result of Y2H assay showed that *Nb*MED10b could directly interact with *Nb*MED7, but not with the other two subunits (Fig. 3*A*). The interaction between *Nb*MED10b and *Nb*MED7 was further confirmed through GST-pull down, Co-IP, and split-luciferase (SLC) assays (Fig. 3 *B* and *C* and *SI Appendix,* Fig. S10*B*).

To determine the role of *NbMED7* in *Sw-5b*-mediated resistance to TSWV infection, we silenced *NbMED7* expression in *Sw-5b* transgenic *N. benthamiana* plants through VIGS (*SI Appendix,* Fig. S11) followed with rub inoculation of TSWV-infected leaf extracts at 21 d post TRV treatment. By 3 d post TSWV-inoculation, the numbers of HR loci and the accumulation level of TSWV RNA in the TSWV-inoculated leaves of the *NbMED7*-silenced plants were significantly lower than those in the TSWV-inoculated leaves of the control plants (Fig. 3 *D* and *E*). In addition, we examined whether silencing *NbMED7* has any effect on TSWV systemic infection in *Sw-5b* transgenic plant. No TSWV systemic infection was detected in the newly merged leaves of the *NbMED7*-silenced plants (Fig. 3 *F* and *G*), indicating that *Nb*MED7 is also an important negative regulator in the *Sw-5b*-mediated resistance to TSWV infection. We generated *Nbmed7* knockout *N. benthamiana* mutant lines. The *Nbmed7* knockout mutant also showed a strong dwarfing phenotype (Fig. 3*H* and *SI Appendix,* Fig. S12). Similar to *Nbmed10b*, the accumulation of TSWV was significantly reduced in *Nbmed7* knockout mutant (Fig. 3*I*).

CC Domain of the Activated Sw-5b Interferes with the Interaction between MED10b and MED7. We conducted yeast three hybrid (Y3H) assay to examine whether Sw-5b CC can interfere with the interaction between *Nb*MED10b and *Nb*MED7 in yeast cells. The result showed that in the presence of Sw-5b CC, but not MBP, the interaction between *Nb*MED10b and *Nb*MED7 was strongly inhibited (Fig. 4*A*). The GST pull-down assay result also showed that when the amount of MBP–Sw-5b-CC was increased, the amount of FLAG-*Nb*MED7 pulled down by GST-*Nb*MED10b was decreased (Fig. 4*B*). In the same assay, the addition of His-MBP had no clear effect on the interaction between GST-*Nb*MED10b and FLAG-*Nb*MED7 (Fig. 4*B*). Co-IP assay confirmed that the interaction between *Nb*MED10b and *Nb*MED7 was significantly reduced in the presence of YFP-Sw-5b-CC but not YFP in vivo (*SI Appendix,* Fig. S13). The Y3H assays and GST pull-down result also showed that Sw-5b CC could interfere with the interaction between *Sl*MED10b and *Sl*MED7 from tomato (*SI Appendix,* Fig. S14 *A* and *B*).

In the absence of TSWV NSm effector, Sw-5b stays in an inactive state and upon recognition of NSm, Sw-5b NLR converts to
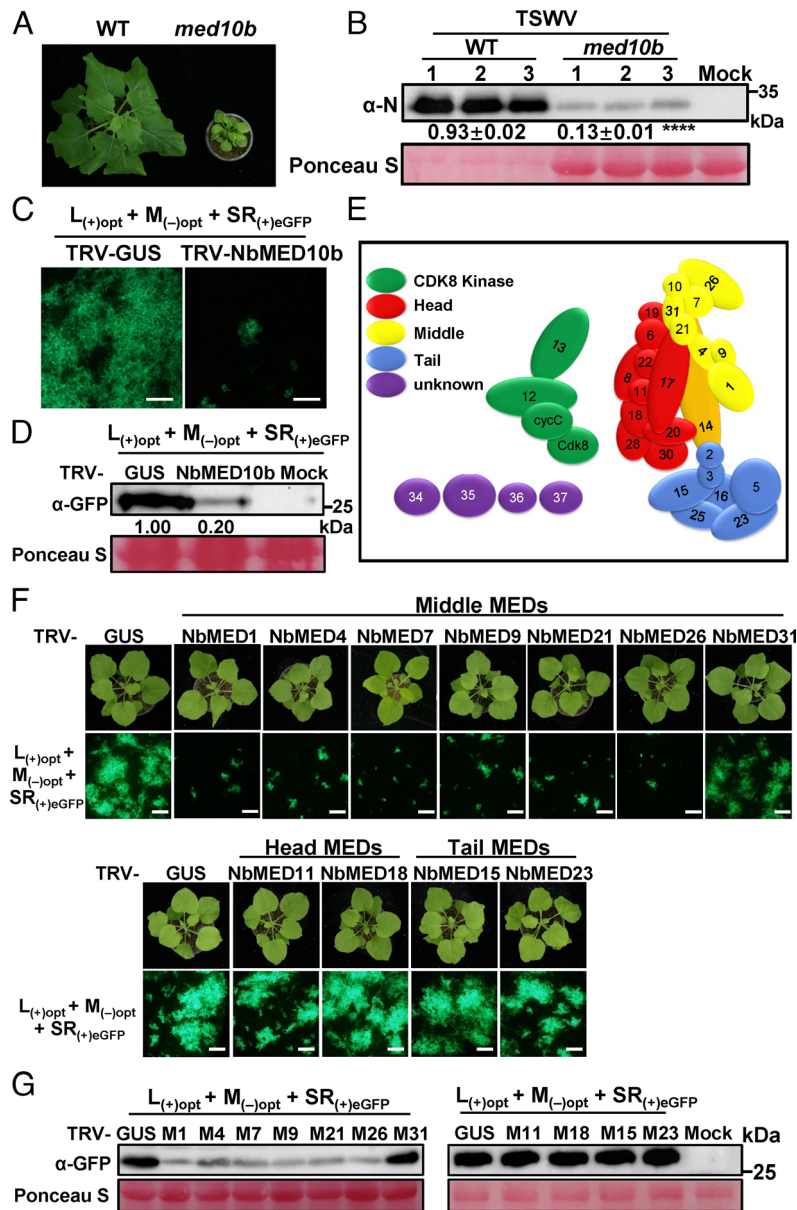
Fig. 2. Knockout/down of *MED10b* and other subunits in the middle module of Mediator complex in wild-type *N. benthamiana* activate plant defense against TSWV infection. (*A*) A photograph showing a 12-wk-old *N. benthamiana* plant and an *Nbmed10b* knockout mutant plant. (*B*) Western blot analysis of TSWV N protein accumulation in the TSWV-inoculated leaves of the wild-type *N. benthamiana* plant or *Nbmed10b* mutant plant at 5 dpi using an N protein–specific antibody. (*C*) *NbMED10b*-silenced (TRV-*NbMED10b*) or nonsilenced (TRV-*GUS* control) *N. benthamiana* plants were inoculated with TSWV infectious clone [L$_{(+)opt}$+M$_{(-)opt}$+SR$_{(+)eGFP}$] via agro-infiltration. The infiltrated *N. benthamiana* plant leaves were harvested at 60 h post-agro infiltration (hpai) and imaged for eGFP fluorescence under an inverted fluorescence microscope (Scale bars, 800 μm.). (*D*) Western blot results showing the accumulation level of eGFP in the infiltrated leaves shown in (*C*) using a GFP-specific antibody at 60 hpai. (*E*) A diagram showing the subunits in the head, middle, and tail modules of Mediator complex in *N. tabacum*. (*F*) Subunits *NbMED1*, *NbMED4*, *NbMED7*, *NbMED9*, *NbMED21*, *NbMED26*, and *NbMED31* in the middle module; subunits *NbMED11* and *NbMED18* in the head module; and subunits *NbMED15* and *NbMED23* in the tail module of Mediator complexes were individually silenced through VIGS using a TRV-based VIGS vector. These *N. benthamiana* plants were then inoculated individually with the TSWV infectious clone L$_{(+)opt}$+M$_{(-)opt}$+SR$_{(+)eGFP}$ via agro-infiltration. The eGFP fluorescence in the inoculated leaves was imaged at 60 h post TSWV inoculation (hpi) under an inverted fluorescence microscope (Scale bars, 800 μm). (*G*) Western blot analysis results showing eGFP accumulations in various assayed leaf samples shown in (*F*) using GFP antibody.

an activated state to trigger defense response (43, 60). To determine which form of Sw-5b could interfere the interaction between *Nb*MED10b and *Nb*MED7, we first performed Y3H assay. The results showed that the full-length autoactive Sw-5b^{D857V}, but not the inactive Sw-5b, reduced the interaction between *Nb*MED10b and *Nb*MED7 (Fig. 4*C*). The activated form of Sw-5b (Sw-5b^{D857V}) also interfered with the interaction between *Nb*MED10b and *Nb*MED7 in vivo (Fig. 4*D*). Western blot analyses showed that the protein accumulations of endogenous *Nb*MED10b and *Nb*MED7 were not affected by the Sw-5b^{D857V} (*SI Appendix,* Fig. S15).

MED10b/MED7 Repress the Expression of Jasmonate-Dependent Defense Response Genes. To further elucidate the downstream components in the CC-induced immune signaling, we used the MED10b or MED7 as the bait to screen its interacting proteins through a Y2H screening. The *Nb*JAZ7, a transcription repressor of JA signaling pathway, was identified to interact with *Nb*MED7 (*SI Appendix,* Fig. S16A). We then examined the interaction of MED7 and MED10b with all 11 members of JAZ proteins from *N. benthamiana* or tomato. *Nb*MED10b does not interact with any of the other JAZ proteins. In addition to *Nb*JAZ7, *Nb*MED7 also interacted with *Nb*JAZ1, *Nb*JAZ2, *Nb*JAZ4,
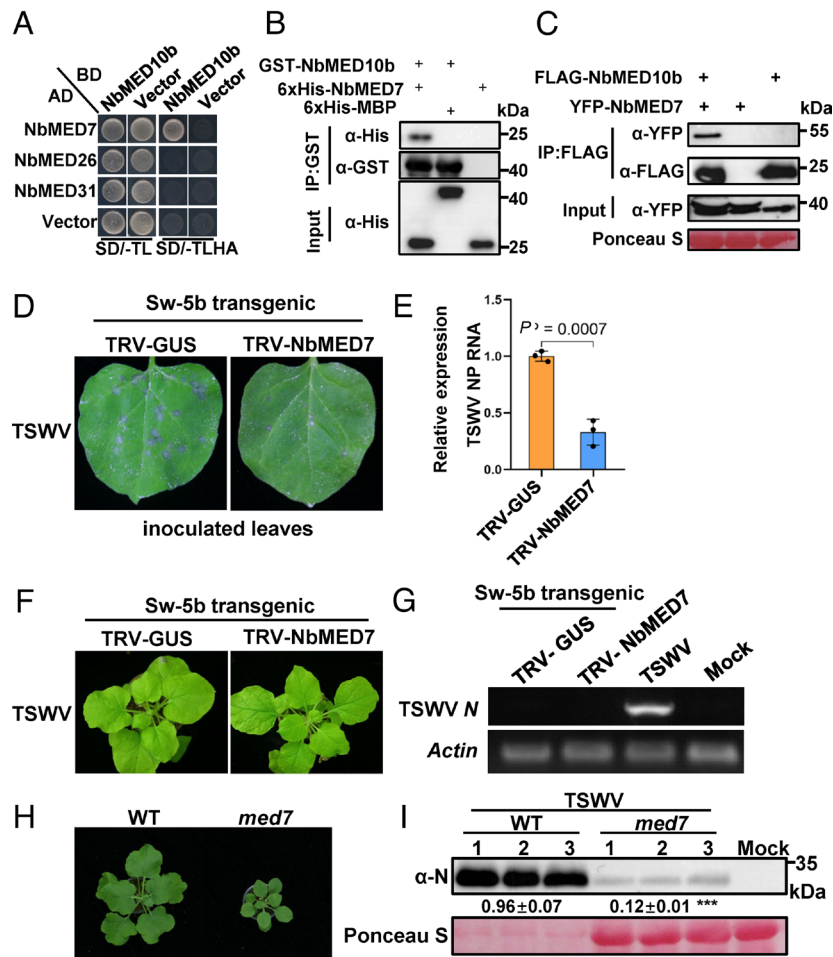
Fig. 3. MED10b interacts with MED7, which also negatively regulates *Sw-5b*-mediated defense. (*A*) A Y2H assay result showing the interaction between *Nb*MED10b and *Nb*MED7, *Nb*MED26, or *Nb*MED31. The transformed yeast cells were grown on the SD/-TL and the SD/-TLHA dropout plates, respectively. (*B*) GST pull-down assay results showing the interaction between the GST-*Nb*MED10b and 6×His-*Nb*MED7. 6×His-*Nb*MED7, 6×His-MBP, and GST-*Nb*MED10b were expressed individually in *E. coli* and then purified. The purified 6×His-*Nb*MED7 or 6×His-MBP was incubated with GST-*Nb*MED10b followed by the pull-down assay using glutathione-sepharose beads. The blots were probed with an anti-GST- or anti-His-specific antibody. (*C*) Co-IP assay results showing the interaction between the FLAG-*Nb*MED10b and YFP-*Nb*MED7. The FLAG-*Nb*MED10b was used to coimmunoprecipitate YFP-*Nb*MED7 from *N. benthamiana* leaf extracts. The blots were probed with an anti-FLAG or an anti-YFP antibody. (*D*) The *Nb*MED7-silenced or nonsilenced *Sw-5b* transgenic *N. benthamiana* plants were inoculated with TSWV-infected crude leaf extracts. The inoculated leaves were photographed at 3 dpi. The number and size of HR loci in these inoculated leaves were determined. (*E*) The accumulation level of TSWV RNA in the inoculated leaves shown in (*D*) was determined through qRT-PCR using the TSWV *N* gene–specific primers at 3 d post TSWV inoculation. The expression levels of *NbActin* in the assayed samples were used as the internal controls. Data are presented as the means ± SE (three biological samples per treatment). (*F*) The TSWV-inoculated *Nb*MED7-silenced or nonsilenced *Sw-5b* transgenic *N. benthamiana* plants were photographed at 14 d post TSWV inoculation. (*G*) Detection of TSWV RNA in the systemic leaves of the TSWV-inoculated *Nb*MED7-silenced or nonsilenced *Sw-5b* transgenic *N. benthamiana* plants through RT-PCR using TSWV *N* gene–specific primers. The systemic leaves of the TSWV-infected *N. benthamiana* plants were used as the positive control. The systemic leaves of the mock-inoculated plants were used as the negative controls. The expression levels of *NbActin* in the assayed samples were used as the internal controls. (*H*) A photograph showing 12-wk-old wild-type *N. benthamiana* plant and an *Nbmed7* knockout mutant plant. (*I*) Western blot analysis of TSWV N protein accumulation in the TSWV-inoculated leaves of the wild-type *N. benthamiana* plant or *Nbmed7* mutant plant at 5 dpi using an N protein–specific antibody.

and *Nb*JAZ9–*Nb*JAZ11 in Y2H assay (Fig. 5*A*). *Sl*MED7 but not *Sl*MED10b also interacts with many *Sl*JAZs (*SI Appendix,* Fig. S16*B*). TPL and NINJA are corepressors of JAZs in JA signaling pathway. Knockout or downregulation of TPL and NINJA can cause the activation of JA signaling (31, 32). We then examined whether the *Nb*MED10b and *Nb*MED7 could interact with *Nb*TPL and *Nb*NINJA. Y2H results showed that neither *Nb*MED10b nor *Nb*MED7 interacts with *Nb*TPL and *Nb*NINJA (*SI Appendix,* Fig. S17).

Next, we examined the JA response genes in *med7* and *med10b* knockout *N. benthamiana* plants. The expression levels of JA response genes *NbAOS*, *NbERF.C3*, and *NbPR-STH2* were significantly up-regulated in both *med7* and *med10b* knockout plants (Fig. 5*B* and *SI Appendix,* Fig. S18*A*). We also examined whether Sw-5b can activate JA signaling pathway upon the recognition of TSWV NSm effector. Coexpression of Sw-5b with NSm significantly up-regulated the expression levels of these JA

response genes but not by coexpression of Sw-5b with EV or NSm with EV (43) (Fig. 5*C* and *SI Appendix,* Fig. S18*B*). Knockdown of a component of the middle Mediator module *NbMED26*, but not *NbMED18* component of the head module or *NbMED23* in the tail module, also up-regulated the expressions of JA response genes (*SI Appendix,* Fig. S18 *C–E*). Knockdown of *SlMED10b* or *SlMED7* also up-regulated the expression levels of JA response genes *SlAOS*, *SlERF.C3*, and *SlPR-STH2* in tomato (*SI Appendix,* Fig. S19 *A* and *B*). Inoculation of TSWV onto tomato cv. IVF3545 (with *Sw-5b*) also activated these JA marker genes (*SI Appendix,* Fig. S19*C*). Transcription factor MYC2 can directly bind to the promoter and activate *LOX2*, a representative JA response gene (61). The addition of *Nb*MYC2 transcription factor strongly activated the luciferase (LUC) reporter gene driven by the *NbLOX2* promoter. However, the addition of *Nb*JAZ1 into *Nb*MYC2 reduced the expression of LUC (Fig. 5*D*). The coaddition of *Nb*MED7 and
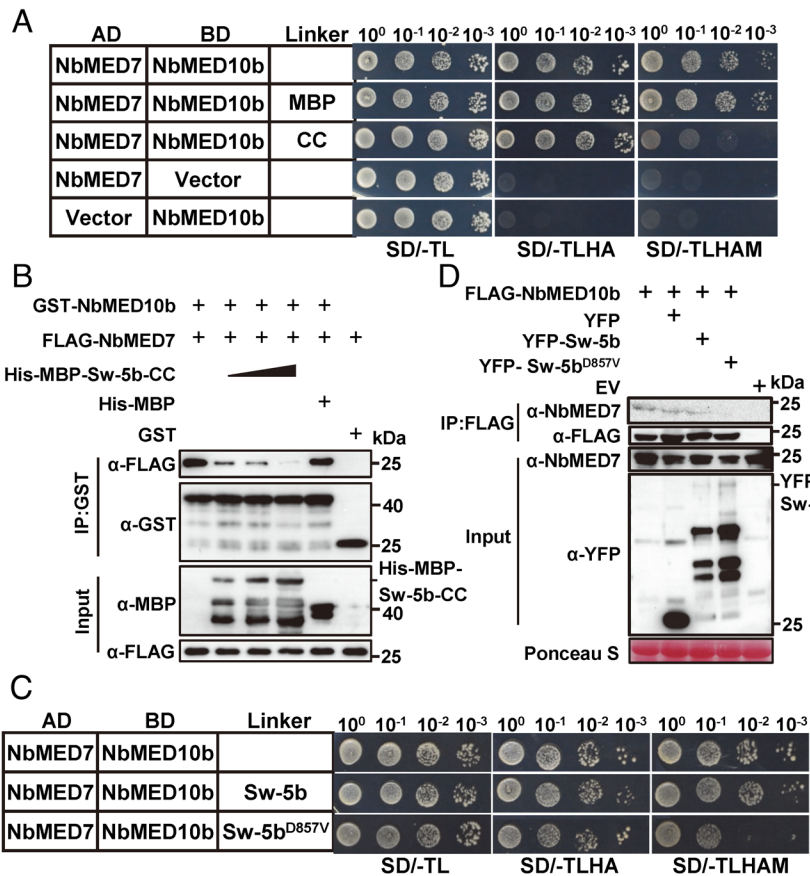
Fig. 4. CC domain of the activated Sw-5b interferes with the interaction between MED10b and MED7. (*A*) Y3H assay results showing the effects of the CC domain on the interaction between *Nb*MED10b and *Nb*MED7. Yeast cells were cotransformed with pGAD-*Nb*MED7 and pBridge-*Nb*MED10b, pGAD-*Nb*MED7 and pBridge-*Nb*MED10b+MBP, or pGAD-*Nb*MED7 and pBridge-*Nb*MED10b + Sw-5b CC domain. The cotransformed yeast cells were grown on the SD/-TL, SD/-TLHA, or SD/-TLHAM (lacking Trp, Leu, His, Ade, and Met) plates, respectively, for 5 d. (*B*) GST pull-down assay results showing the effect of Sw-5b CC domain on the interaction between *Nb*MED10b and *Nb*MED7. Fixed amount of GST-MED10b and FLAG-MED7 was incubated with increasing amounts of purified His-MBP–Sw-5b-CC or purified His-MBP protein (control). Proteins in the samples were then pulled down using glutathione-sepharose beads followed by western blot assays with an anti-GST-, anti-MBP-, or anti-FLAG-specific antibody. (*C*) Y3H assay results showing that the full-length Sw-5b^D857V, but not Sw-5b, interrupted the interaction between *Nb*MED10b and *Nb*MED7. Yeast cells were cotransformed with constructs expressing AD-*Nb*MED7 + BD-*Nb*MED10b + empty vector, AD-*Nb*MED7 + BD-*Nb*MED10b + Sw-5b, or AD-*Nb*MED7 + BD-*Nb*MED10b + Sw-5b^D857V. The transformed cells were grown on the SD/-TL, SD/-TLHA, and SD/-TLHAM plates, respectively, to assess the *Nb*MED7 and *Nb*MED10b interaction. (*D*) FLAG-*Nb*MED10b was used to immunoprecipitate the endogenous *Nb*MED7 in *N. benthamiana* leaves in the presence of YFP, YFP-Sw-5b, and YFP-Sw-5b^D857V, respectively. Western blots were probed using an anti-FLAG, anti-YFP, or anti-*Nb*MED7 antibody.

*Nb*JAZ1 to *Nb*MYC2 further inhibited the expression of LUC. The coexpression of *Nb*MED7, *Nb*MED10b, and *Nb*JAZ1 inhibited the expression of LUC further more (Fig. 5*E*), while the coexpression of *Nb*MED10b and *Nb*JAZ1 without *Nb*MED7 did not further reduce the expression of LUC (*SI Appendix,* Fig. S20*A*). Moreover, the coexpression of *Nb*MED7, *Nb*MED10b, *Nb*MED26, *Nb*MED31, and *Nb*JAZ1 with *Nb*MYC2 completely suppressed the expression of LUC (Fig. 5*E*). These effects on *LOX2* promoter were not observed in the absence of JAZ1 (*SI Appendix,* Fig. S20*B*), suggesting that MED7/MED10b work together with JAZ1 to suppress the transcription of JA response genes. Next, we tested whether Sw-5b can derepress the inhibitory effect of JAZ1–MED7–MED10b. The results showed that coexpression of Sw-5b and NSm caused fluorescence quenching and no LUC expression was detected (*SI Appendix,* Fig. S20*C*). However, the addition of Sw-5b CC activated the expression of LUC, suggesting that Sw-5b CC can derepress JAZ1–MED7–MED10b-mediated repression of JA-dependent transcription (Fig. 5*F*). Furthermore, we investigated the role of MED7/MED10b repression and Sw-5b derepression on plant resistance to TSWV (*SI Appendix,* Fig. S21 *A* and *B*). The results showed that coexpression of the transcription factor *Nb*MYC2 with TSWV infectious clones L$_{(+)opt}$+M$_{(-)opt}$+SR$_{(+)eGFP}$ reduced the expression of the TSWV eGFP reporter. Coexpression of *Nb*MED7, *Nb*MED10b, and *Nb*JAZ1 attenuated the inhibitory effect of MYC2 on TSWV reporter accumulation. However, coexpression of Sw-5b or Sw-5b CC with *Nb*MYC2, *Nb*JAZ1, *Nb*MED7, and *Nb*MED10b strongly inhibited TSWV accumulation in *N. benthamiana* leaves. We have shown recently that exogenous application of JA induces defense against TSWV (62). Here, we further treated the wild-type *N. benthamiana* with MeJA followed by inoculation of TSWV L$_{(+)opt}$+M$_{(-)opt}$+SR$_{(+)eGFP}$ infectious clones via agro-infiltration. The results further showed that the JA treatment

significantly inhibited TSWV infection in *N. benthamiana* (Fig. 5 *G* and *H*).

CC Domain of Various Other CNLs from Solanaceae Modulates MED10b/MED7 Interaction to Activate Jasmonate-Dependent Immune Pathway. We next investigated whether CC domain of other CNLs from *Solanaceae* (Fig. 6*A*) has effect on MED10b and MED7 interaction. Y2H and BiFC assay results showed that the CC domains of Mi-1.2, Rpi-blb2, Rpi-vnt1, R3a, Prf, and Rx were all capable of interacting with *Nb*MED10b (Fig. 6*B* and *SI Appendix,* Fig. S22). The TIR domain of tobacco NLR N was, however, incapable of interacting with *Nb*MED10b in yeast (Fig. 6*B*). We then cloned *Sl*MED10b from tomato and *St*MED10b from potato and tested their abilities to interact with the CC domains described above. As shown in *SI Appendix,* Fig. S23 *A* and *B*, *Sl*MED10b did interact with the CC domains of Mi-1.2 and Prf, whereas *St*MED10b interacted with the CC domains of Rpi-blb2, Rpi-vnt1, R3a, and Rx. Based on these findings, we conclude that MED10bs in various solanaceous species can interact with the CC domains of NLR receptors. Besides the CC domains of sensor NLRs, *Nb*MED10b also interacted strongly with the CC domains of helper NLRs *Nb*NRC2a, *Nb*NRC2b, and *Nb*NRC3 and weakly with the CC domain of *Nb*NRC4 (Fig. 6*C*). *Nb*MED10b, however, did not interact with the CC domains of helper NLRs *Nb*NRG1 and *Nb*ADR1 (Fig. 6*C*).

Next, we used Y3H assay to test the abilities of different CC domains to disrupt the interaction between MED7 and MED10b. The results showed that the CC domains of sensor (Fig. 6*D*) and helper NLRs (Fig. 6*E*) that interact with *Nb*MED10b could all reduce the *Nb*MED7 and *Nb*MED10b interaction. In addition, the Y3H assay results showed that the CC domains of these solanaceous NLRs could disrupt the interaction between *Sl*MED7 and *Sl*MED10b or the interaction between *St*MED7 and *St*MED10b
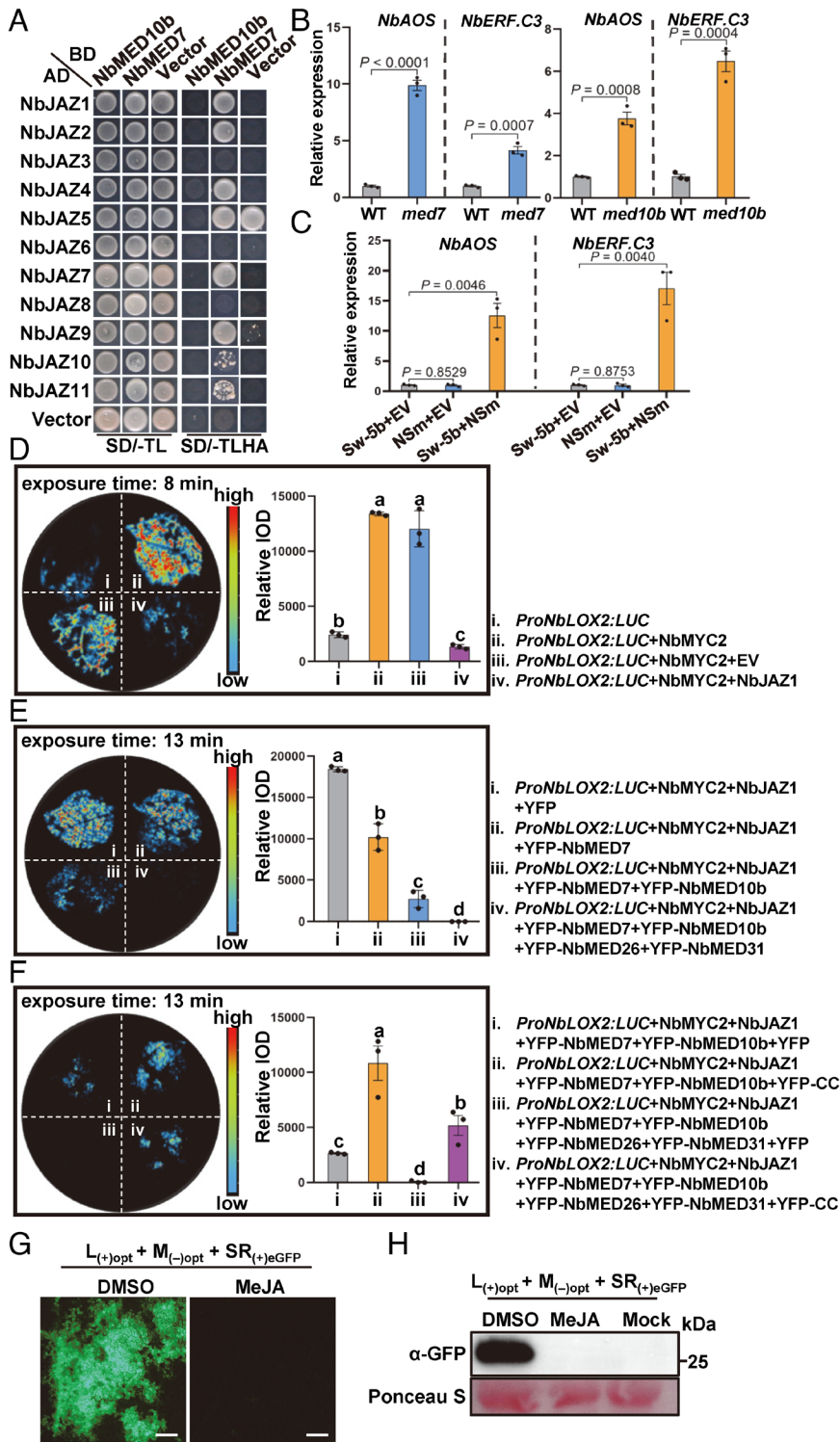
Fig. 5. MED10b/MED7 mediate jasmonate-dependent transcription repression. (*A*) A Y2H assay result showing the interaction between *Nb*JAZs and *Nb*MED10b or between *Nb*JAZs and *Nb*MED7. The transformed yeast cells were grown on the SD/-TL and the SD/-TLHA plates, respectively. (*B*) Quantitative RT-PCR analysis results showing the expressions of representative marker genes involved in the JA signaling pathways in wild-type (WT) *N. benthamiana Nbmed7* knockout, and the *Nbmed10b* knockout plants. The expression levels of *NbActin* in these samples were used as the internal controls. Data are presented as the means ± SE (three independent biological sample per treatment). (*C*) Quantitative RT-PCR analysis results showing the expressions of representative marker genes involved in the JA signaling pathways in *N. benthamiana* coexpressing Sw-5b with EV, NSm with EV, or Sw-5b with NSm. The expression levels of *NbActin* in these samples were used as the internal controls. Data are presented as the means ± SE (three independent biological samples per treatment). (*D*) Transient overexpression of *Nb*MYC2 transcription factor activated the expression of luciferase (LUC) driven by the *NbLOX2* promoter, and addition of *Nb*JAZ1 into *Nb*MYC2 reduced the expression of LUC. The luciferase activity (integrated optical density, IOD) in the treated leaves was quantified and shown in the right. Data are presented as the means ± SE (three independent biological samples per treatment). (*E*) Coexpression of *Nb*JAZ1, or *Nb*MED7 and *Nb*JAZ1, or *Nb*MED7, *Nb*MED10b, and *Nb*JAZ1, or *Nb*MED7, *Nb*MED10b, *Nb*MED26, *Nb*MED31, and *Nb*JAZ1 with *Nb*MYC2 reduced the expression of LUC. The luciferase activity (integrated optical density, IOD) in the treated leaves was quantified and shown in the right. Data are presented as the means ± SE (three independent biological samples per treatment). (*F*) Coexpression of Sw-5b CC with *Nb*MYC2, *Nb*JAZ1, *Nb*MED7 and *Nb*MED10b, or *Nb*MYC2, *Nb*JAZ1, *Nb*MED7, *Nb*MED10b, *Nb*MED26, and *Nb*MED31 activated the expression of LUC. The luciferase activity (integrated optical density, IOD) in the treated leaves was quantified and shown in the right. Data are presented as the means ± SE (three independent biological samples per treatment). (*G*) *N. benthamiana* plants were sprayed with DMSO or 100 μM MeJA. At 2 d post treatment, phytohormone-treated leaves were inoculated again with TSWV infectious clone [L(+)opt+M(−)opt+SR(+)eGFP] via agro-infiltration. The infiltrated *N. benthamiana* plant leaves were harvested at 60 hpai and imaged for eGFP fluorescence loci under an inverted fluorescence microscope (Scale bars, 800 μm.). (*H*) Western blot assay results showing the accumulation level of eGFP at 60 hpai in the infiltrated leaves shown in (*G*), using GFP antibody.

(*SI Appendix,* Fig. S23 *C and D*). The GST pull-down assay results confirmed that MBP–Mi-1.2-CC or MBP–Rpi-blb2-CC interfered with the interactions between *Nb*MED7 and *Nb*MED10b, *Sl*MED7 and *Sl*MED10b, or *St*MED7 and *St*MED10b (*SI Appendix,* Fig. S24 *A–D*). GST pull-down assays also showed that the addition of His-MBP–*Nb*NRC2a-CC or His-MBP–*Nb*NRC3-CC reduced the interaction between *Nb*MED7 and *Nb*MED10b (*SI Appendix,* Fig. S25 *A and B*).

Next, we investigated whether Rx, Rpi-blb2, or Mi-1.2 can activate JA signaling pathway upon the recognition of corresponding effector protein or when NLR switched into an active form.

Coexpression of Rx and PVX or Rpi-blb2 and Avr-blb2 significantly up-regulated the expression levels of JA response genes *NbAOS, NbERF.C3,* and *NbPR-STH2* but not by the expression of Rx or Rpi-blb2 alone (Fig. 6 *F* and *G* and *SI Appendix,* Fig. S26 *A* and *B*). Similarly, the autoactive Mi-1.2^T557S mutant (63) also up-regulated the expression levels of these JA response genes (Fig. 6*H* and *SI Appendix,* Fig. S26*C*).

Because the CC domains of various NLRs in *Solanaceae* could interfere with the interaction between MED7 and MED10b, we also investigated whether downregulation of MED10b and MED7 activates the host resistance against different pathogens. As *med10b* and
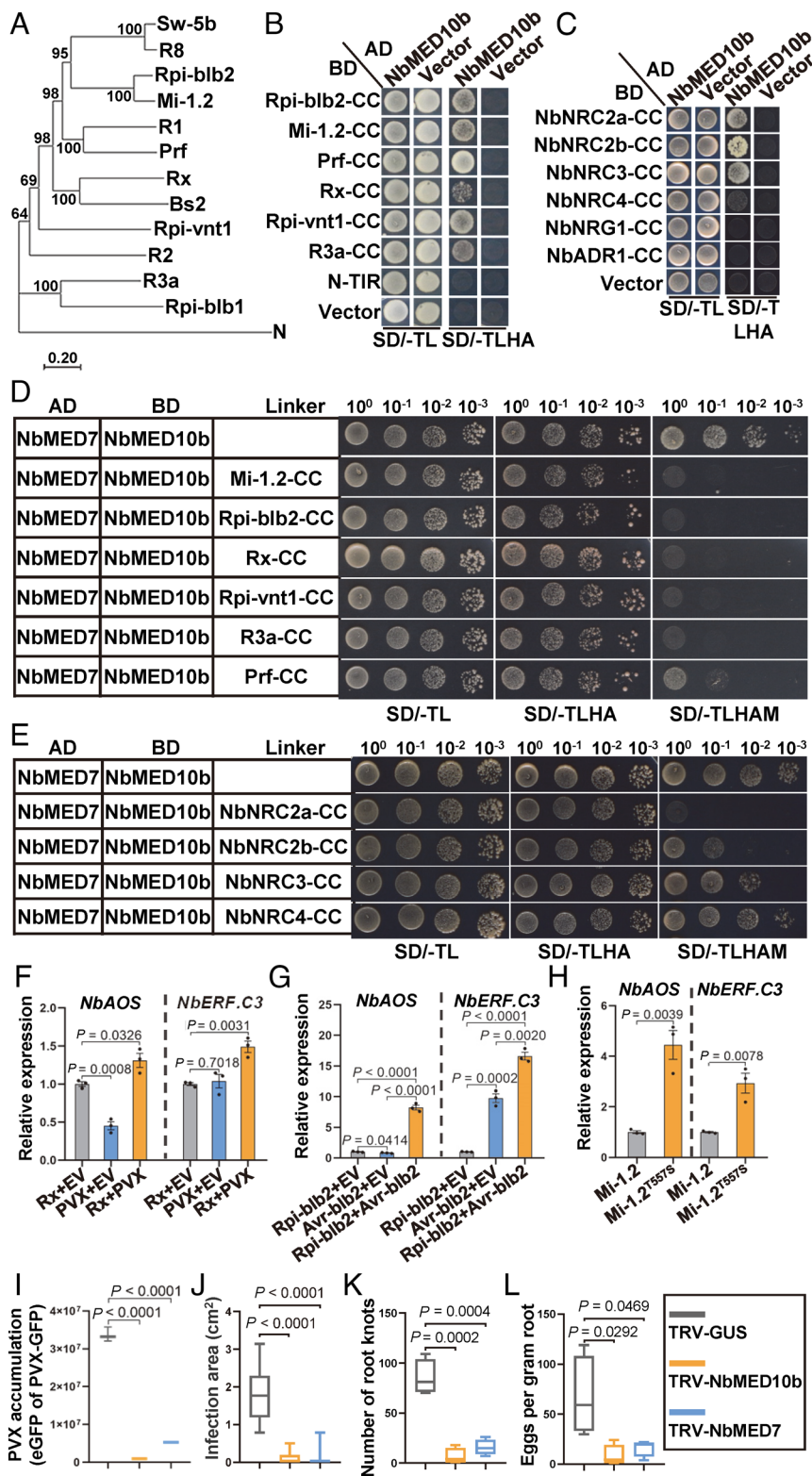
Fig. 6. CC domain of CNLs in *Solanaceae* modulates MED10b/MED7 interaction to activate jasmonate-dependent immune pathway. (*A*) A phylogenetic tree constructed using CNLs from various solanaceous species. Sequences of these NLRs were retrieved from the GenBank, and the phylogenetic tree was conducted using the neighbor-joining method in the MEGA7 package. (*B*) Y2H assay results showing the interactions between *Nb*MED10b and various CC domains of CNLs from different solanaceous species. The transformed yeast cells were grown on the SD/-TL and the SD/-TLHA plates, respectively. (*C*) Y2H assay results showing the interactions between *Nb*MED10b and the CC domains in the helper NLRs NRC2/3/4. The transformed yeast cells were grown on the SD/-TL and the SD/-TLHA plates, respectively. (*D*) Y3H assay results showing the effects of CC domains from different CC-type NLRs on the interaction between *Nb*MED10b and *Nb*MED7. Yeast cells coexpressing AD-*Nb*MED7, BD-*Nb*MED10b, Mi-1.2-CC, Rip-blb2-CC, Rx-CC, Rpi-vnt1-CC, R3a-CC, or Prf-CC were grown, respectively, on the SD/-TL, SD/-TLHA, or SD/-TLHAM medium plates to determine the interaction between *Nb*MED7 and *Nb*MED10b. (*E*) Y3H assay results showing the effects of the CC domains of NRC2a, NRC2b, NRC3, and NRC4 on the interaction between *Nb*MED10b and *Nb*MED7. Yeast cells coexpressing AD-*Nb*MED7, BD-*Nb*MED10b, Vector, *Nb*NRC2a-CC, *Nb*NRC2b-CC, *Nb*NRC3-CC, or *Nb*NRC4-CC were grown on the SD/-TL, SD/-TLHA, or SD/-TLHAM medium plates to determine the interaction between *Nb*MED7 and *Nb*MED10b. (*F*) Quantitative RT-PCR analysis results showing the expressions of representative marker genes involved in the JA signaling pathways in *N. benthamiana* coexpressing Rx with EV, PVX with EV, or Rx with PVX. The expression levels of *NbActin* in these samples were used as the internal controls. Data are presented as the means ± SE (three independent biological samples per treatment). (*G*) Quantitative RT-PCR analysis results showing the expression of representative marker genes involved in the JA signaling pathways in *N. benthamiana* coexpressing Rpi-blb2 with EV, Avr-blb2 with EV, or Rpi-blb2 with Avr-blb2. The expression levels of *NbActin* in these samples were used as the internal controls. Data are presented as the means ± SE (three independent biological samples per treatment). (*H*) Quantitative RT-PCR analysis results showing the expressions of representative marker genes involved in the JA signaling pathways in *N. benthamiana* expression of Mi-1.2 or Mi-1.2^{T557S}. The expression levels of *NbActin* in these samples were used as the internal controls. Data are presented as the means ± SE (three independent biological samples per treatment). (*I*) The accumulation level of eGFP expressing from PVX in *NbMED10b*-silenced, *NbMED7*-silenced, or nonsilenced control (TRV-*GUS*) leaves of *N. benthamiana* in the infiltrated leaves was measured and quantified using the Image J software. Statistical analyses were done using the two-tailed Student's *t* test. Data are presented as the means ± SE (three biological samples per treatment). (*J*) The size of *P. infestans* lesions in *NbMED10b*-silenced, *NbMED7*-silenced, or nonsilenced control leaves of *N. benthamiana* was measured and quantified using the Image J software. Statistical analyses were done using the two-tailed Student's *t* test. Data are presented as the means ± SE (10 biological samples per treatment). (*K*) The numbers of root knots on *NbMED10b*-silenced, *NbMED7*-silenced, or nonsilenced control (TRV-*GUS*) roots of *N. benthamiana* plants and the statistical differences between the treatments were determined using the two-tailed Student's *t* test. Data are presented as the means ± SE (four biological samples per treatment). (*L*) The numbers of nematode egg masses on the assayed plant roots. The statistical differences between the treatments were determined using the two-tailed Student's *t* test. Data are presented as the means ± SE (four biological samples per treatment).

med7 knockout plant grow too small to perform these experiments, we silenced the expression of *NbMED10b* and *NbMED7* in *N. benthamiana* plants through VIGS using TRV-*NbMED10b* and TRV-*NbMED7*, respectively (*SI Appendix,* Fig. S27 *A* and *B*). The gene silenced or nonsilenced control plants were inoculated with PVX-GFP, *P. infestans,* or *M. incognita*. Compared to the control plants (TRV-*GUS*), silencing of *NbMED10b* or *NbMED7* expression in *N. benthamiana* plants strongly inhibited PVX-GFP infection (Fig. 6*I* and *SI Appendix,* Fig. S27 *C* and *D*) and *P. infestans* infection (Fig. 6*J* and *SI Appendix,* Fig. S27*E*). The *NbMED10b*- or

NbMED7-silenced *N. benthamiana* plants also showed a strong resistance to *M. incognita* infection. The numbers of *M. incognita*-induced root knots or egg masses in the roots of the *NbMED10b*- or *NbMED7*-silenced plants were significantly reduced compared to the nonsilenced control plants (Fig. 6 *K* and *L* and SI Appendix, Fig. S27*F*). These results show that *Nb*MED10b and *Nb*MED7 function as negative regulators of CNL-mediated immunity in *Solanaceae*.

Discussion

In this study, we demonstrate that MED10b/MED7 mediate jasmonate-dependent transcription repression, and CC domains of CNLs from *Solanaceae* derepress the repressor activity of MED10b–MED7–JAZ and activate immunity. Using Sw-5b NLR as a model, we show that Sw-5b CC domain directly interacts with MED10b. Knockout/down subunits including MED10b and MED7 cause the activation of defense against TSWV. MED10b was found to directly interact with MED7, whereas MED7 directly interacts with JAZ transcription repressor proteins. MED10b–MED7–JAZ proteins together can strongly corepress the expression of JA defense response genes. However, Sw-5b CC interferes with the interaction between MED10b and MED7, and consequently derepresses the corepressor activity of MED10b–MED7–JAZ, leading to the activation of JA-dependent defense response against TSWV infection. Furthermore, using various other CNLs from *Solanaceae*, we show that the CC domains of those CNLs including helper NLR NRCs can also modulate MED10b/MED7 to activate defense against different pathogens.

NINJA (NOVEL INTERACTOR OF JAZ) and TPL (TOPLESS) were previously shown to serve as corepressors of JAZ proteins in JA pathway (31, 32). Our findings reveal that MED10b and MED7 proteins serve as previously unknown repressors of jasmonate-dependent transcription through interaction with JAZ proteins. MED7 was found to directly interact with JAZ proteins. Coexpression of MED10b, MED7, JAZ, and other middle Mediator module components together can strongly cosuppress the expression of JA response genes. This corepression is dependent on JAZ proteins. It was previously shown that knockout of either NINJA or TPL activates JA signaling pathway (31). It was also reported that transcription corepressor TPL interacts with AtMED21 and AtMED10a in *Arabidopsis*, and this interaction is necessary for TPL to function as a corepressor in Auxin signaling (64). In this study, knockout/down of MED10b, MED7, and other subunits can activate the JA pathway, and it mediates defense response against TSWV. Furthermore, knockdown subunits in the head and tail modules of Mediator do not lead to the activation of JA response genes, suggesting that subunits in the middle module mainly participate in the repression function. Together, we propose that MED10b–MED7–JAZ and other subunits of the middle module may form a complex, and this entire supercomplex functions as a repressor of JA response genes. Knockout/down of either MED10b, MED7, or TPL in this supercomplex repressor possibly disrupt the complex formation and hence lead to activation of JA-specific defense response.

The Mediator complex in eukaryotes serves as a molecular bridge to link specific enhancer-bound transcription factors to RNA polymerase II to engage in the initiation of gene transcription/activation (22, 23). Our results suggest that the entire middle module of the Mediator complex may function as a corepressor of JAZ proteins in JA pathway. How can the Mediator complex act both as a corepressor and a molecular linker to activate downstream JA defense genes? It has been reported previously that the transcriptional corepressor TPL forms a bridge between IAA14 and the CKM component MED13 through the physical interaction.

Auxin induces the dissociation of MED13 from the ARF7-binding region upstream of its target gene (65). These findings indicate that auxin induced compositional change in the Mediator in ARF7- and ARF19-mediated transcription. Chen and colleagues recently reported that the mammalian Mediator complex has several different conformations (66). The biological significance of these conformations remains unclear. We speculate that these different conformations may have distinct functions in gene transcription regulations. For instance, one form of Mediator complex acts as a corepressor to inhibit JA defense gene expressions through physical interaction of subunits in the middle module with transcription repressor JAZs and corepressor TPL. When its conformation changes to another form, it functions as a molecular bridge to connect specific transcription factor(s) to Pol II and consequently activates JA-dependent defense gene expressions. These conformation changes are perhaps the most economical way to recruit and bridge the Mediator complexes with Pol II during host defense responses. When JA pathway was not activated, the subunits in the middle module physically interact with JAZs, TPL, and Mediator, which maybe already on the transcription factors but act as a corepressor. Upon triggering the activation of JA pathway, the JAZs are degraded or the MED10b/MED7 interaction is disturbed, either of which may change the conformation of the Mediator from a repressor into a molecular bridge to connect between MYC2/3/4 transcription factors and Pol II. This role of the Mediator may specifically act in stress response, as it needs to respond quickly to environmental clues. Further studies are needed to elucidate the substantial role and mechanism underlying Mediator complex conformational changes in regulating defense gene repression and activation.

Recent studies have demonstrated an important role of JA signaling in plant defense against various pathogens including viruses (34). In this study, we showed that coexpression of Sw-5b NLR and NSm elicitor activated the JA signaling. Consistent with this, the application of JA significantly reduced TSWV infection in *N. benthamiana* and in pepper plants (62). Activation of the JA signaling pathway was also found in another tomato NLR gene, *Sl5R-1*, which also confers resistance to TSWV and was map cloned recently (67). The expression levels of JA response genes *SlMYC2, SlJAZ, SlAOC,* and *SlAOS* were significantly up-regulated in TSWV-inoculated *Sl5R-1* resistant plants compared to noninoculated resistant plants. In contrast, these genes were down-regulated in susceptible plants. The NLRs that confer the resistance to bacteria typically activate salicylic acid (SA) signaling rather than JA signaling. Consistent with this, SA, but not JA, is critical for regulating plant defense against bacterial infection. Interestingly, we found here that coexpression of potato NLR Rpi-blb2 and Avr-blb2 from *Phytophthora* up-regulated the JA response genes. Recently, exogenous application of JA has been shown to improve plant resistance to *Phytophthora* (68). The tomato NLR Mi-1.2 confers the resistance to nematode and the constitutive mutant Mi-1.2^{T557S} can also activate JA signaling. It has been previously reported that JA application reduces nematode reproduction on tomato plants (69).

Previous studies have identified some proteins that interact with NLRs to activate downstream immune signaling (49–53, 70–72). Interestingly, the CC domain of barley CNL MLA has been shown to interact with HvWRKY1 or HvWRKY2, and this interaction derepresses the inhibitory effect of HvWRKY1 or HvWRKY2 on plant defense (49). However, those protein-mediated immune signaling pathways are usually used by specific NLR. In this study, we show that different CNLs in the family of *Solanaceae* can interact with MED10b and consequently interfere with the interaction between MED10b and MED7. This
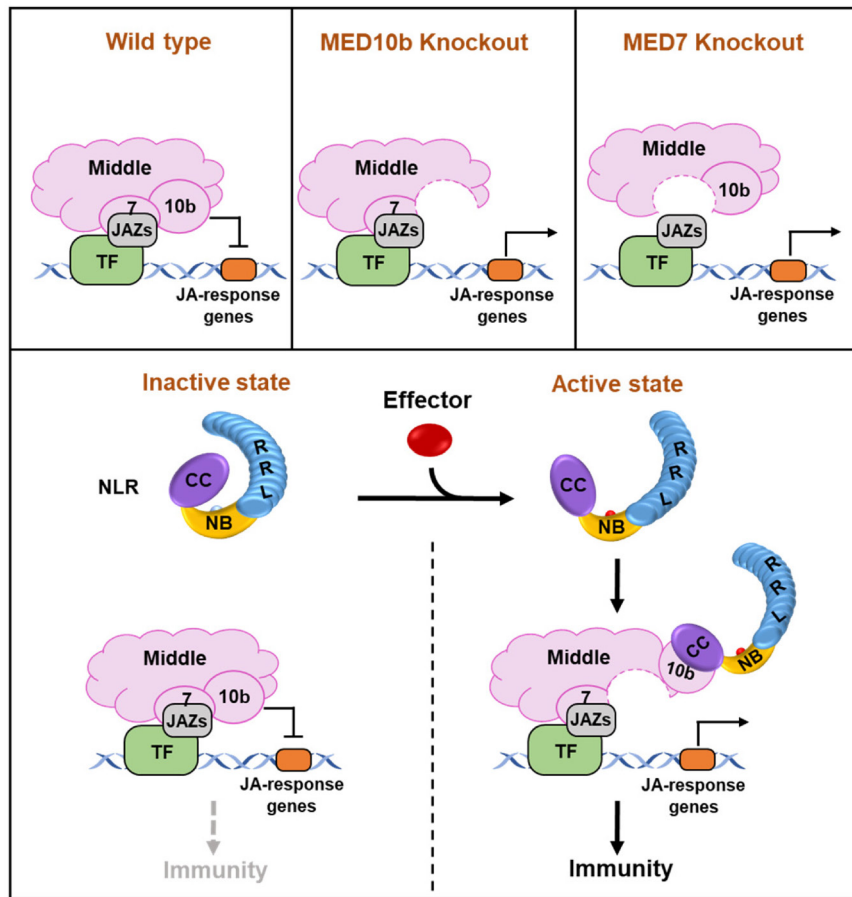
Fig. 7. A model describing the role of MED10b/MED7 in the middle module of Mediator complex as corepressors of JA defense signaling. Knockout MED10b or MED7 derepresses the corepressor activity of the middle module on JA defense gene expression. Upon recognition of pathogen effectors, the CC containing NLRs switch from an inactive state into an activate state and the CC domain of the activated NLRs binds to MED10b. This binding interferes with MED10b and MED7 association and derepresses the MED7–MED10b–JAZ-mediated repression on JA-dependent gene transcription, thus leading to the activation of plant immunity to different pathogens.

suggests that derepression of repressor activities of MED10–MED7 in the middle module of Mediator complex might be a conserved mechanism used by diverse CNLs in the family of *Solanaceae* to activate immune pathway. The helper NLR NRCs can also interfere with MED10b and MED7 interaction; therefore, the helper NLRs might further amplify the expressions of JA signaling–dependent defense genes through derepressing the corepressor activities of MED10b/MED7.

Based on these findings, we propose that the MED10b, MED7, and other subunits in the middle module of Mediator complex function as corepressors for JA defense signaling through MED7 and JAZ interaction (Fig. 7). Knockout of MED10b or MED7 derepresses the corepressor activity of the middle module on JA defense gene expression. Upon recognition of pathogen effectors, the CNLs switch from an inactive state into an active state and the CC domain of the active CNLs binds to MED10b. This binding interferes with the MED10b and MED7 association and derepresses the MED7–MED10b–JAZ-mediated repression on JA-dependent gene transcription, thus leading to the activation of plant immunity to different pathogens (Fig. 7).

Materials and Methods

Details of the methodology used are provided in *SI Appendix*, Materials and Methods, and include plant material and growth conditions, plasmid construction, HR assay, Y2H assay, Y3H assay, VIGS assay, virus inoculation, total RNA extraction, RT-PCR, qRT-PCR, antibody production, coimmunoprecipitation assay, protein expression, protein purification, GST pull-down assay, BiFC assay, SLC

complementation assay, CRISPR/Cas9 technology, inoculation of *P. infestans* assay, trypan blue staining assay, nematode inoculation assay, quantification, and statistical analysis. Primers used in this study are listed in *SI Appendix,* Table S1.

Data, Materials, and Software Availability. All study data are included in the article and/or *SI Appendix*.

Author affiliations: aThe Key Laboratory of Plant Immunity, Department of Plant Pathology, Nanjing Agricultural University, Nanjing 210095, P. R. China; bSalinity Agriculture Research Laboratory, Jiangsu Coastal Area Institute of Agricultural Sciences, Yancheng 224002, P. R. China; cInstitute of Biotechnology, Zhejiang University, Hangzhou 310058, P. R. China; dInstitute of Vegetables and Flowers, Chinese Academy of Agricultural Sciences, Beijing 100081, P. R. China; eInstitute of Horticulture Science, Shanghai Academy of Agricultural Sciences, Shanghai 201403, P. R. China; fYunnan Academy of Tobacco Agricultural Sciences, Key Laboratory of Tobacco Biotechnological Breeding, National Tobacco Genetic Engineering Research Center, Kunming 650021, P. R. China; gYunnan Provincial Key Laboratory of Agri-Biotechnology, Institute of Biotechnology and Genetic Resources, Yunnan Academy of Agricultural Sciences, Kunming, Yunnan 650223, P. R. China; and hDepartment of Plant Biology and The Genome Center College of Biological Sciences, University of California, Davis, CA 95616

1. J. D. Jones, J. L. Dangl, The plant immune system. *Nature* **444**, 323–329 (2006).
2. J. D. Jones, R. E. Vance, J. L. Dangl, Intracellular innate immune surveillance devices in plants and animals. *Science* **354**, aaf6395 (2016).
3. D. Couto, C. Zipfel, Regulation of pattern recognition receptor signalling in plants. *Nat. Rev. Immunol.* **16**, 537–552 (2016).
4. J. M. Zhou, Y. Zhang, Plant immunity: Danger perception and signaling. *Cell* **181**, 978–989 (2020).
5. X. Yu, B. M. Feng, P. He, L. B. Shan, From chaos to harmony: Responses and signaling upon microbial pattern recognition. *Annu. Rev. Phytopathol.* **55**, 109–137 (2017).
6. H. Cui, K. Tsuda, J. E. Parker, Effector-triggered immunity: From pathogen perception to robust defense. *Annu. Rev. Plant Biol.* **66**, 487–511 (2015).
7. J. Caplan, M. Padmanabhan, S. P. Dinesh-Kumar, Mant NB-LRR immune receptors: From recognition to transcriptional reprogramming. *Cell Host Microbe* **3**, 126–135 (2008).
8. Y. Peng, R. van Wersch, Y. Zhang, Convergent and divergent signaling in PAMP-triggered immunity and effector-triggered immunity. *Mol. Plant Microbe Interact.* **31**, 403–409 (2018).
9. K. Tsuda, F. Katagiri, Comparing signaling mechanisms engaged in pattern-triggered and effector-triggered immunity. *Curr. Opin. Plant Biol.* **13**, 459–465 (2010).
10. B. P. M. Ngou, H. K. Ahn, P. Ding, J. D. G. Jones, Mutual potentiation of plant immunity by cell-surface and intracellular receptors. *Nature* **592**, 110–115 (2021).
11. M. Yuan *et al.*, Pattern-recognition receptors are required for NLR-mediated plant immunity. *Nature* **592**, 105–109 (2021).
12. X. Zhang, P. N. Dodds, M. Bernoux, What do we know about NOD-like receptors in plant immunity? *Annu. Rev. Phytopathol.* **55**, 205–229 (2017).
13. F. L. Takken, W. I. Tameling, To nibble at plant resistance proteins. *Science* **324**, 744–746 (2009).
14. F. Monteiro, M. T. Nishimura, Structural, functional, and genomic diversity of plant NLR proteins: An evolved resource for rational engineering of plant immunity. *Annu. Rev. Phytopathol.* **56**, 243–267 (2018).
15. G. Bi *et al.*, The ZAR1 resistosome is a calcium-permeable channel triggering plant immune signaling. *Cell* **184**, 3528–3541.e3512 (2021).
16. J. Wang *et al.*, Reconstitution and structure of a plant NLR resistosome conferring immunity. *Science* **364**, 5868–5870 (2019).
17. S. J. Huang *et al.*, Identification and receptor mechanism of TIR-catalyzed small molecules in plant immunity. *Science* **377**, 487 (2022).
18. A. L. Jia *et al.*, TIR-catalyzed ADP-ribosylation reactions produce signaling molecules for plant immunity. *Science* **377**, 488 (2022).
19. P. Jacob *et al.*, Plant "helper" immune receptors are Ca(2+)-permeable nonselective cation channels. *Science* **373**, 420–425 (2021).
20. A. Kunstler, R. Bacso, G. Gullner, Y. M. Hafez, L. Kiraly, Staying alive–Is cell death dispensable for plant disease resistance during the hypersensitive response? *Physiol. Mol. Plant Pathol.* **93**, 75–84 (2016).
21. X. Chen *et al.*, A multilayered regulatory mechanism for the autoinhibition and activation of a plant CC-NB-LRR resistance protein with an extra N-terminal domain. *New Phytol.* **212**, 161–175 (2016).
22. Y. J. Kim, S. Bjorklund, Y. Li, M. H. Sayre, R. D. Kornberg, A multiprotein mediator of transcriptional activation and its interaction with the C-terminal repeat domain of RNA polymerase II. *Cell* **77**, 599–608 (1994).
23. R. D. Kornberg, Mediator and the mechanism of transcriptional activation. *Trends Biochem. Sci.* **30**, 235–239 (2005).
24. J. A. Davis, Y. Takagi, R. D. Kornberg, F. A. Asturias, Structure of the yeast RNA polymerase II holoenzyme: Mediator conformation and polymerase interaction. *Mol. Cell* **10**, 409–415 (2002).
25. F. C. Holstege *et al.*, Dissecting the regulatory circuitry of a eukaryotic genome. *Cell* **95**, 717–728 (1998).
26. B. L. Allen, D. J. Taatjes, The mediator complex: A central integrator of transcription. *Nat. Rev. Mol. Cell Biol.* **16**, 155–166 (2015).
27. B. N. Kidd, D. M. Cahill, J. M. Manners, P. M. Schenk, K. Kazan, Diverse roles of the mediator complex in plants. *Semin. Cell Dev. Biol.* **22**, 741–748 (2011).
28. M. Buendia-Monreal, C. S. Gillmor, Mediator: A key regulator of plant development. *Dev. Biol.* **419**, 7–18 (2016).
29. J. Browse, Jasmonate passes muster: A receptor and targets for the defense hormone. *Annu. Rev. Plant Biol.* **60**, 183–205 (2009).
30. C. Wasternack, B. Hause, Jasmonates: Biosynthesis, perception, signal transduction and action in plant stress response, growth and development. An update to the 2007 review in annals of botany. *Ann. Bot.* **111**, 1021–1058 (2013).
31. L. Pauwels *et al.*, NINJA connects the co-repressor TOPLESS to jasmonate signalling. *Nature* **464**, 788–791 (2010).
32. F. Zhang *et al.*, Structural basis of JAZ repression of MYC transcription factors in jasmonate signalling. *Nature* **525**, 269–273 (2015).
33. A. P. Kloek *et al.*, Resistance to pseudomonas syringae conferred by an arabidopsis thaliana coronatine-insensitive (coi1) mutation occurs through two distinct mechanisms. *Plant J.* **26**, 509–522 (2001).
34. R. Li *et al.*, Jasmonate-based warfare between the pathogenic intruder and host plant: Who wins?. *J. Exp. Bot.* **74**, 1244–1257 (2023).
35. J. H. Qiu *et al.*, Warm temperature compromises JA-regulated basal resistance to enhance magnaporthe oryzae infection in rice. *Mol. Plant* **15**, 723–739 (2022).
36. M. F. Ji *et al.*, Turnip mosaic virus P1 suppresses JA biosynthesis by degrading cpSRP54 that delivers AOCs onto the thylakoid membrane to facilitate viral infection. *Plos Pathog.* **17**, e1010108 (2021).
37. Y. Q. He *et al.*, Jasmonic acid-mediated defense suppresses brassinosteroid-mediated susceptibility to rice black streaked dwarf virus infection in rice. *New Phytol.* **214**, 388–399 (2017).
38. J. L. Hu *et al.*, Rice stripe virus suppresses jasmonic acid-mediated resistance by hijacking brassinosteroid signaling pathway in rice. *Plos Pathog.* **16**, e1008801 (2020).
39. L. L. Li *et al.*, A class of independently evolved transcriptional repressors in plant RNA viruses facilitates viral infection and vector feeding. *Proc. Natl. Acad. Sci. U.S.A.* **118**, e2016673118 (2021).
40. K. B. Scholthof *et al.*, Top 10 plant viruses in molecular plant pathology. *Mol. Plant Pathol.* **12**, 938–954 (2011).
41. H. R. Pappu, R. A. Jones, R. K. Jain, Global status of tospovirus epidemics in diverse cropping systems: Successes achieved and challenges ahead. *Virus Res.* **141**, 219–236 (2009).
42. J. E. Oliver, A. E. Whitfield, The genus tospovirus: Emerging bunyaviruses that threaten food security. *Annu. Rev. Virol.* **3**, 101–124 (2016).
43. M. Zhu *et al.*, The intracellular immune receptor Sw-5b confers broad-spectrum resistance to tospoviruses through recognition of a conserved 21-amino acid viral effector epitope. *Plant Cell* **29**, 2214–2232 (2017).
44. M. Zhu, I. L. van Grinsven, R. Kormelink, X. R. Tao, Paving the way to tospovirus infection: Multilined interplays with plant innate immunity. *Annu. Rev. Phytopathol.* **57**, 41–62 (2019).
45. S. H. Brommonschenkel, A. Frary, A. Frary, S. D. Tanksley, The broad-spectrum tospovirus resistance gene Sw-5 of tomato is a homolog of the root-knot nematode resistance gene Mi. *Mol. Plant Microbe Interact.* **13**, 1130–1138 (2000).
46. M. I. Spassova *et al.*, The tomato gene Sw5 is a member of the coiled coil, nucleotide binding, leucine-rich repeat class of plant resistance genes and confers resistance to TSWV in tobacco. *Mol. Breeding* **7**, 151–161 (2001).
47. A. Bombarely *et al.*, A draft genome sequence of nicotiana benthamiana to enhance molecular plant-microbe biology research. *Mol. Plant Microbe Interact.* **25**, 1523–1530 (2012).
48. C. H. Wu *et al.*, NLR network mediates immunity to diverse plant pathogens. *Proc. Natl. Acad. Sci. U.S.A.* **114**, 8113–8118 (2017).
49. Q. H. Shen *et al.*, Nuclear activity of MLA immune receptors links isolate-specific and basal disease-resistance responses. *Science* **315**, 1098–1103 (2007).
50. C. Chang *et al.*, Barley MLA immune receptors directly interfere with antagonistically acting transcription factors to initiate disease resistance signaling. *Plant Cell* **25**, 1158–1173 (2013).
51. L. Hu *et al.*, The coiled-coil and nucleotide binding domains of brown planthopper resistance 14 function in signaling and resistance against planthopper in rice. *Plant Cell* **29**, 3157–3185 (2017).
52. K. Zhai *et al.*, RRM transcription factors interact with NLRs and regulate broad-spectrum blast resistance in rice. *Mol. Cell* **74**, 996–1009.e1007 (2019).
53. H. Inoue *et al.*, Blast resistance of CC-NB-LRR protein Pb1 is mediated by WRKY45 through protein-protein interaction. *Proc. Natl. Acad. Sci. U.S.A.* **110**, 9577–9582 (2013).
54. M. Feng *et al.*, Rescue of tomato spotted wilt virus entirely from complementary DNA clones. *Proc. Natl. Acad. Sci. U.S.A.* **117**, 1181–1190 (2020).
55. T. Koschubs *et al.*, Preparation and topology of the mediator middle module. *Nucleic Acids Res.* **38**, 3186–3195 (2010).
56. H. Chen *et al.*, Cytoplasmic and nuclear Sw-5b NLR act both independently and synergistically to confer full host defense against tospovirus infection. *New Phytol.* **231**, 2262–2281 (2021).
57. A. Bendahmane, K. Kanyuka, D. C. Baulcombe, The Rx gene from potato controls separate virus resistance and cell death responses. *Plant Cell* **11**, 781–792 (1999).
58. M. R. Hajimorad, J. H. Hill, Rsv1-mediated resistance against soybean mosaic virus-N is hypersensitive response-independent at inoculation site, but has the potential to initiate a hypersensitive response-like mechanism. *Mol. Plant Microbe Interact.* **14**, 587–598 (2001).
59. Q. Zhai, C. Li, The plant mediator complex and its role in jasmonate signaling. *J. Exp. Bot.* **70**, 3415–3424 (2019).
60. J. Li *et al.*, A plant immune receptor adopts a two-step recognition mechanism to enhance viral effector perception. *Mol. Plant* **12**, 248–262 (2019).
61. Y. You, Q. Zhai, C. An, C. Li, LEUNIG_HOMOLOG mediates MYC2-dependent transcriptional activation in cooperation with the coactivators HAC1 and MED25. *Plant Cell* **31**, 2187–2205 (2019).
62. J. Chen *et al.*, NLR surveillance of pathogen interference with hormone receptors induces immunity. *Nature* **613**, 145–152 (2023).
63. S. H. Gabriels *et al.*, An NB-LRR protein required for HR signalling mediated by both extra- and intracellular resistance proteins. *Plant J.* **50**, 14–28 (2007).
64. A. R. Leydon *et al.*, Repression by the arabidopsis TOPLESS corepressor requires association with the core mediator complex. *Elife* **10**, e66739 (2021).
65. J. Ito *et al.*, Auxin-dependent compositional change in mediator in ARF7- and ARF19-mediated transcription. *Proc. Natl. Acad. Sci. U.S.A.* **113**, 6562–6567 (2016).
66. X. Chen *et al.*, Structures of the human mediator and mediator-bound preinitiation complex. *Science* **372**, abg0635 (2021).
67. S. Qi *et al.*, A new NLR gene for resistance to tomato spotted wilt virus in tomato (Solanum lycopersicum). *Theor. Appl. Genet.* **135**, 1493–1509 (2022).
68. Y. Zhao *et al.*, The phytophthora effector Avh94 manipulates host jasmonic acid signaling to promote infection. *J. Integr. Plant Biol.* **64**, 2199–2210 (2022).
69. W. R. Cooper, L. Jia, L. Goggin, Effects of jasmonate-induced defenses on root-knot nematode infection of resistant and susceptible tomato cultivars. *J. Chem. Ecol.* **31**, 1953–1967 (2005).
70. M. S. Padmanabhan *et al.*, Novel positive regulatory role for the SPL6 transcription factor in the N TIR-NB-LRR receptor-mediated plant innate immunity. *PLoS Pathog.* **9**, e1003235 (2013).
71. Z. Zhu *et al.*, Arabidopsis resistance protein SNC1 activates immune responses through association with a transcriptional corepressor. *Proc. Natl. Acad. Sci. U.S.A.* **107**, 13960–13965 (2010).
72. F. El Kasmi, How activated NLRs induce anti-microbial defenses in plants. *Biochem. Soc. Trans.* **49**, 2177–2188 (2021).